Building and Environment, Vol. 12, pp. 251–261. Pergamon Press 1977. Printed in Great Britain

Dynamic Torsional Coupling in Asymmetric Building Structures

ANDREI REINHORN*
AVIGDOR RUTENBERG†
JACOB GLÜCK‡

An approximate method is proposed for the dynamic analysis of torsionally coupled tall building structures by utilizing the properties of their uncoupled counterparts. An exact solution is first given for the particular case in which the lateral and torsional stiffness matrices are uncoupled by same transformation. The method is then applied to a wider class of structures where this condition is only approximately satisfied by reducing the dynamic coupling problem to an approximate two-degrees-of-freedom system. Simple formulae and graphical representations of dynamic magnification of static eccentricity are given. Two numerical examples illustrate the use of the proposed method, checking on its accuracy and comparing its results with seismic code provisions.

NOMENCLATURE

The following symbols are used in this paper:

a	distance between elastic centers KC and SC
a_{ij}	perturbation coefficients
$\mathbf{C}$	damping matrix
C_j	modal eccentricity amplification factor
E	Young's Modulus
e	static eccentricity
e_d	dynamic eccentricity
H	height of building
h	story's height
I	unit diagonal matrix
I_x, I_y	second moment of area about x and y axes respectively
I_ω	second sectorial moment
i	mass radius of giration
K	stiffness matrix
L_x, L_y	plan dimensions of building
M	mass matrix
N	number of reference levels
P	equivalent coupled force
P_c	uncoupled lateral force
p_i	static eigenvalues
q	modal amplitude
r_k, r_s	radii of gyration for k and s system respectively
r	direction vector $[\mathbf{r}^T = (1, 1, 1, \ldots, 0, 0, 0, \ldots)]$
S	stiffness matrix
S_a	acceleration spectrum
S_d	displacement spectrum
T	equivalent torsional moment
$\ddot{u}_g$	ground acceleration time history
$\mathbf{v}$	displacement response vector
α	noncoupled modal shapes ratio
Γ_j	modal participation factor
Γ_s	static participation matrix
γ	static eigenvector component
ε	perturbation factor
ε_j	correction coefficient
$\mathbf{\Phi}$	modal shape matrix
$\boldsymbol{\phi}$	mode shape vector
$\mathbf{K}$	stiffness matrix
λ	eigenvalue
$\mathfrak{M}$	mass matrix
$\mu, \Delta\mu$	mass matrices
ω	natural frequency
ω'	damped natural frequency
$\mathbf{\Psi}$	coupling shape matrix
$\boldsymbol{\psi}$	coupling shape vector
ξ	damping ratio.
Subscripts	
L	lateral components
R	rotational components
o	noncoupled values.

*Instructor, Faculty of Civil Engineering, Technion—Israel Institute of Technology, Haifa, Israel.
†Senior Lecturer, Faculty of Civil Engineering, Technion—Israel Institute of Technology, Haifa, Israel.
‡Associate Professor, Faculty of Civil Engineering, Technion—Israel Institute of Technology, Haifa, Israel.

INTRODUCTION

THE TORSIONAL response of building structures to earthquake excitation is of increasing concern to structural engineers. Three main torsional effects are well recognized: accidental eccentricity, torsional ground motion and coupling between lateral and rotational vibrations. This last effect which characterizes buildings with asymmetric layout of the structural components with respect to the floor plan is the subject of this study.

The behavior of single story asymmetric structures under lateral earthquake excitation has been extensively studied. Apparently, Housner and Outinen[6] were the first to point out that the static method of analysis underestimates significantly the maximum stresses in such structures. The effect of coupling, especially when the lateral and torsional frequencies are close, was investigated by Bustamente and Rosenblueth[2], Skinner *et al.*[18], Rosenblueth and Elorduy[15], Keintzel[10] and very recently by Kan and Chopra[9]. These studies led to the realization that if the static methods of analysis are to continue in use, statically computed eccentricities should be amplified. Accordingly several seismic codes[7] adopted simple formulae to allow for this effect. The limitations inherent in the RSS (root-sum-square) formula for combining the spectral values in the modal analysis [e.g. (12)] were also recognized in these studies[2, 15, 18]. Techniques to overcome these difficulties by means of two-degree-of-freedom response spectra were proposed by Penzien[13, 14].

The dynamic behavior of asymmetric multistory buildings has not been as thoroughly studied. Bustamente and Rosenblueth[2] analyzed a large number of such buildings in which static eccentricities were assigned to some or all floors. On the basis of their study they concluded that a rough estimate of torsional effects could be obtained from the response of single story structures with similar characteristics. Skinner *et al.*[18] suggested that the dynamic properties of asymmetric multistory buildings could be derived from those of similar but symmetric buildings and those of single story asymmetric structures, provided certain requirements were satisfied. These requirements consist of geometrical similarity of all floor plans, centers of stiffness (elastic centers) and of gravity located on two vertical axes, constant values of radii of inertia and stiffness, plus certain other limitations on the structural type. The two axes requirement is also given by Penzien[13], apparently without any further qualifications.

A technique whereby the dynamic properties of asymmetric multistory structures can be derived from those of their symmetric counterparts and those of two-degree-of-freedom (2-d.f.) systems, is likely to reduce the computational effort appreciably. Moreover, if the natural frequencies of the 2-d.f. systems are close, then the results may be used directly as input for the 2-d.f. response spectrum analysis developed by Penzien[13, 14] or for the amplification curves given by Rosenblueth and Elorduy[12, 15]. The purpose of the present paper is to present a general approach to the study of torsionally coupled building structures by using the properties of their uncoupled counterparts, thereby extending the scope of the methods used by Rosenblueth and Elorduy[15] and by Penzien[13, 14] to structures which may not have an elastic center. This approach is also a generalization of the techniques used in an earlier paper[17] for evaluating the natural frequencies and mode shapes of uniform asymmetric wall-frame structures. The details developed herein are for a floor plan with one axis of symmetry so that torsional coupling is confined to one axis only, but the method as presented is also applicable to the more general case with no axis of symmetry. An exact solution satisfying the uncoupling requirements is first given for the special case in which the lateral and torsional stiffness matrices are uncoupled by the same transformation. The method is then applied to a wider class of structures where this condition is only approximately satisfied. Graphical presentations of the dynamic magnification of static eccentricity for certain structural types are given in the paper and permit a rapid evaluation of the seismic response. The paper closes with two numerical examples illustrating the use of the proposed method, checking on its accuracy and comparing its results with seismic code provisions. It is believed that the proposed approach will lead to a better understanding of the nature of the lateral torsional coupling effect and hopefully will contribute to a more rational treatment of dynamic amplification in earthquake code provisions.

ANALYTICAL MODEL

The representation of torsional coupling in asymmetric structures by means of 2-d.f. systems is carried out for two basic models. The first is a building in which the mass centers of the floors are located on one vertical axis throughout the height (point MC in Fig. 1) and the elastic centers are located on another vertical axis (point KC in Fig. 1[19, 20]. The second model is a building with two types of framing systems. Each system comprises several vertical planar assemblages having similar stiffness properties (e.g. frames or flexural walls) and a common variation thereof along the height. The elastic centers of these systems and the mass centers are located on three different vertical axes (points KC, SC and MC respectively in Fig. 2). It is apparent that no single center of

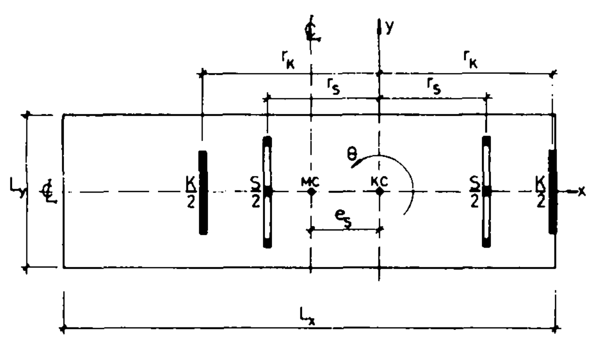

Fig. 1. Typical floor plan Asymmetric structure: First model.

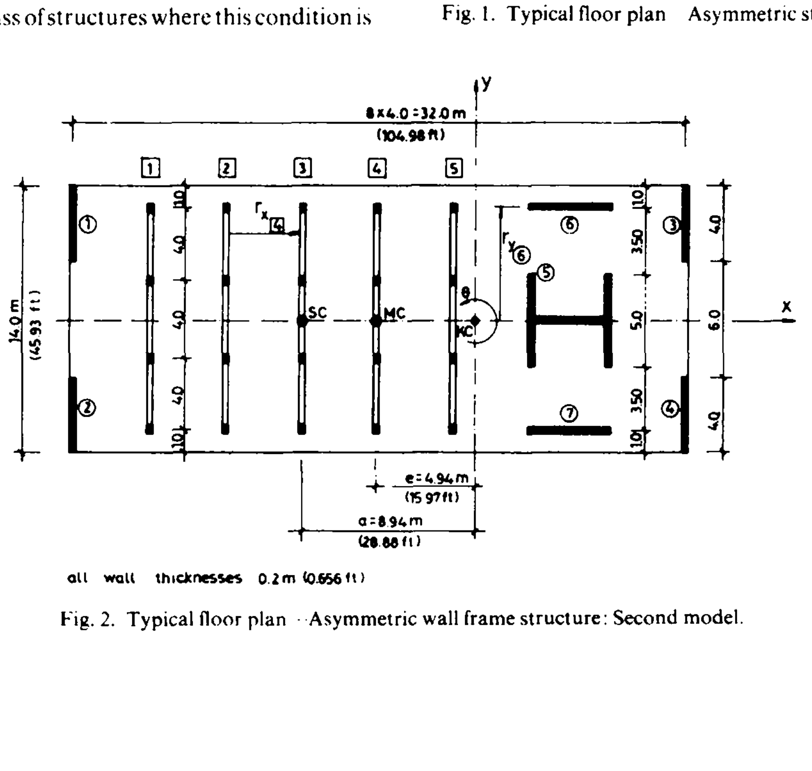

Fig. 2. Typical floor plan—Asymmetric wall frame structure: Second model.

rigidity can be defined for this model. These two models represent, at least approximately, a wide class of high-rise building structures.

Considering the first model, the dynamic properties of the vibrating system are obtained from the solution of the free vibration equation

$$(\mathbf{K} - \omega^2 \mathfrak{M})\boldsymbol{\phi} = 0 \tag{1}$$

or:

$$\left(\begin{bmatrix} K_L & 0 \\ 0 & K_R \end{bmatrix} - \omega^2 \begin{bmatrix} M & Me \\ Me & M(e^2+i^2) \end{bmatrix}\right) \cdot \begin{Bmatrix} \boldsymbol{\phi}_L \\ \boldsymbol{\phi}_R \end{Bmatrix} = \begin{Bmatrix} \mathbf{0} \\ \mathbf{0} \end{Bmatrix} \tag{1a}$$

in which K_L and K_R are respectively the lateral and torsional stiffness matrices of order N about the elàstic center KC, M = the diagonal mass matrix, $\boldsymbol{\phi}_L$ and $\boldsymbol{\phi}_R$ = lateral and torsional components of the mode shapes, ω = the natural frequency, e = eccentricity of mass center MC from KC, and i = mass radius of gyration about MC, assumed to be constant. Methods of assembling K_L and K_R from the individual structural assemblages of beams, columns and walls are well known (e.g.[4, 19]) and will not be discussed here. As will be shown subsequently, under certain conditions the $2N \times 2N$ eigenproblem in equation (1) may be uncoupled into N, 2-d.f. systems, thereby considerably simplifying the problem. Let ω_{Lo} and $\boldsymbol{\phi}_{Lo}$ be the solutions of the eigenproblem:

$$(K_L - \omega_{Lo}^2 M)\phi_{Lo} = 0 \tag{2}$$

and let ω_{Ro} and $\boldsymbol{\phi}_{Ro}$ be the solution of

$$(K_R - \omega_{Ro}^2 \cdot M \cdot i^2)\boldsymbol{\phi}_{Ro} = 0 \tag{3}$$

in which $\omega_{Lo}, \omega_{Ro}, \boldsymbol{\phi}_{Lo}$ and $\boldsymbol{\phi}_{Ro}$ are the natural frequencies and mass normalized mode shapes respectively of the uncoupled $N \times N$ systems of equations (2, 3). Expressing the normal mode shapes $\boldsymbol{\phi}$ [equation (1)] in terms of the modal coordinates $\boldsymbol{\phi}_{Lo}$ and $\boldsymbol{\phi}_{Ro}$:

$$\begin{Bmatrix} \boldsymbol{\phi}_L \\ \boldsymbol{\phi}_R \end{Bmatrix} = \begin{bmatrix} \boldsymbol{\Phi}_{Lo} & 0 \\ 0 & \boldsymbol{\Phi}_{Ro} \end{bmatrix} \begin{Bmatrix} \boldsymbol{\psi}_L \\ \boldsymbol{\psi}_R \end{Bmatrix} = \boldsymbol{\Phi}_o \boldsymbol{\psi} \tag{4}$$

in which $\boldsymbol{\Phi}_{Lo}$ and $\boldsymbol{\Phi}_{Ro}$ are the modal matrices of $\boldsymbol{\phi}_{Lo}$ and $\boldsymbol{\phi}_{Ro}$, substituting in equation (1), premultiplying by $\boldsymbol{\Phi}_0^T$ (T designates the transpose) and using the orthogonality properties, the following expression is obtained:

$$\left(\begin{bmatrix} \omega_{Lo}^2 & 0 \\ 0 & \omega_{Ro}^2 \end{bmatrix} - \omega^2 \begin{bmatrix} I & \boldsymbol{\Phi}_{Lo}^T M i \boldsymbol{\Phi}_{Ro} \cdot e/i \\ \boldsymbol{\Phi}_{Ro}^T M_i \boldsymbol{\Phi}_{Lo} \cdot e/i & I[1+(e/i)^2] \end{bmatrix}\right) \begin{Bmatrix} \boldsymbol{\psi}_L \\ \boldsymbol{\psi}_R \end{Bmatrix} = \begin{Bmatrix} \mathbf{0} \\ \mathbf{0} \end{Bmatrix} \tag{5}$$

in which ω_{Lo}^2 and ω_{Ro}^2 are the diagonal matrices of ω_{Lo}^2 and ω_{Ro}^2 respectively. To uncouple equation (5) into N 2-d.f. equations it is required that:

$$\boldsymbol{\Phi}_{Lo} \equiv \boldsymbol{\Phi}_{Ro} \cdot i \tag{6}$$

so that the off-diagonal matrices in the second matrix equation (5) become diagonal. This condition is satisfied when:

$$K_L K_R = K_R K_L. \tag{7}$$

Then equation (5) takes the form:

$$\left(\begin{bmatrix} \omega_{Lo}^2 & 0 \\ 0 & \omega_{Ro}^2 \end{bmatrix} - \omega^2 \begin{bmatrix} I & I \cdot e/i \\ I \cdot e/i & I[1+(e/i)^2] \end{bmatrix}\right) \begin{Bmatrix} \boldsymbol{\psi}_L \\ \boldsymbol{\psi}_R \end{Bmatrix} = \begin{Bmatrix} \mathbf{0} \\ \mathbf{0} \end{Bmatrix} \tag{8}$$

and it is readily seen that equation (8) is equivalent to N 2×2 matrix equations of the form:

$$\left(\begin{bmatrix} \omega_{Loj}^2 & 0 \\ 0 & \omega_{Roj}^2 \end{bmatrix} - \omega_j^2 \begin{bmatrix} 1 & e/i \\ e/i & 1+(e/i)^2 \end{bmatrix}\right) \cdot \begin{Bmatrix} \psi_{Lj} \\ \psi_{Rj} \end{Bmatrix} = \begin{Bmatrix} 0 \\ 0 \end{Bmatrix} \tag{9}$$

which upon solution of the quadratic characteristic equation yields the natural frequencies:

$$\left(\frac{\omega_{1,2}^2}{\omega_{Lo}^2}\right)_j = \frac{1}{2}\left[1 + \left(\frac{e}{i}\right)^2 + \left(\frac{\omega_{Ro}^2}{\omega_{Lo}^2}\right)_j \pm \sqrt{\left[1 + \left(\frac{e}{i}\right)^2 - \left(\frac{\omega_{Ro}^2}{\omega_{Lo}^2}\right)_j\right]^2 + 4\left(\frac{e}{i}\right)^2 \cdot \left(\frac{\omega_{Ro}^2}{\omega_{Lo}^2}\right)_j}\,\right] \tag{10}$$

and the mode shapes

$$\begin{Bmatrix} \psi_{L_n} \\ \psi_{R_n} \end{Bmatrix}_j = \frac{1}{\left[1 - \left(\frac{\omega_n^2}{\omega_{Lo}^2}\right)_2\right]^2 + \left(\frac{e}{i}\right)^2} \begin{Bmatrix} \frac{a}{i} \cdot \left(\frac{\omega_n^2}{\omega_{Lo}^2}\right)_j \\ 1 - \left(\frac{\omega_n^2}{\omega_{Lo}^2}\right)_j \end{Bmatrix} \quad (n = 1, 2). \tag{11}$$

Equation (9) is the 2-d.f. model used by Skinner *et al.*[17], Rosenblueth and Elorduy[15] and Penzien[13, 14], and it is evident that it is strictly applicable to eccentric multistory buildings in which the mass centers and the elastic centers are located along two vertical axes only when equation (7) is satisfied.

Although in general equation (6) is not exactly satisfied, so that $\boldsymbol{\Phi}_{Lo}^T \cdot M \cdot i \cdot \boldsymbol{\Phi}_{Ro}$ and $\boldsymbol{\Phi}_{Ro}^T \cdot M \cdot i \cdot \boldsymbol{\Phi}_{Lo}$ are not diagonal, yet an approximate solution may be obtained by neglecting the off-diagonal terms of these matrices. Before discussing the accuracy of this approximation it will be shown that the behavior of the second model described earlier in this section may also be expressed in the form of equation (5) and thus be amenable to the same approximate solution.

Using KC as the reference axis, the free vibration equation for the second model reads:

$$\left(\begin{bmatrix} K_L & 0 \\ 0 & K_L \cdot r_K^2 \end{bmatrix} + \begin{bmatrix} S_L & S_L \cdot a \\ S_L \cdot a & S_L(a^2 + r_S^2) \end{bmatrix} - \omega^2 \begin{bmatrix} M & M \cdot e \\ M \cdot e & M(e^2 + i^2) \end{bmatrix}\right) \cdot \begin{Bmatrix} \phi_L \\ \phi_R \end{Bmatrix}_{KC} = \begin{Bmatrix} \mathbf{0} \\ \mathbf{0} \end{Bmatrix} \quad (12)$$

in which S_L = lateral stiffness matrix of the second framing system, a = distance from its elastic center to KC, r_K and r_S = radii of gyration of K_L and S_L about KC and SC respectively (Fig. 2). Now it is possible to transform equation (12) into the form of equation (1) by means of the eigenvalues $p_{1,2}^2$ and the eigenvectors of the 2-d.f. system[16]:

$$\left(\begin{bmatrix} 1 & a/r_K \\ a/r_K & (a/r_K)^2 + (r_S/r_K)^2 \end{bmatrix} - p^2 \begin{bmatrix} 1 & 0 \\ 0 & 1 \end{bmatrix}\right) \cdot \begin{Bmatrix} 1 \\ \gamma \end{Bmatrix} = \begin{Bmatrix} 0 \\ 0 \end{Bmatrix} \quad (13)$$

that is:

$$\begin{Bmatrix} \phi_L \\ \phi_R \end{Bmatrix}_{KC} = \frac{1}{1+\gamma^2} \begin{bmatrix} I & -I \cdot \gamma \\ I \cdot \gamma & I \end{bmatrix} \begin{Bmatrix} \phi_L \\ \phi_R \end{Bmatrix} = \mathbf{\Gamma}_S \begin{Bmatrix} \phi_L \\ \phi_R \end{Bmatrix} \quad (14)$$

which in turn leads to:

$$(\mathbf{K}^* - \omega^2 \mathfrak{M}^*)\boldsymbol{\phi} = 0 \quad (15)$$

or

$$\left(\begin{bmatrix} K_L + p_1^2 S_L & 0 \\ 0 & K_L + p_2^2 S_L \end{bmatrix} - \omega^2 \cdot \begin{bmatrix} M^* & M^* e^* \\ M^* e^* & M^*(e^{*2} + i^{*2}) \end{bmatrix}\right) \begin{Bmatrix} \phi_L \\ \phi_R \end{Bmatrix} = \begin{Bmatrix} \mathbf{0} \\ \mathbf{0} \end{Bmatrix} \quad (15a)$$

in which

$$p_{1,2}^2 = \frac{1}{2}\left[1 + \left(\frac{a}{r_K}\right)^2 + \left(\frac{r_s}{r_K}\right)^2 \pm \sqrt{\left[1 + \left(\frac{a}{r_K}\right)^2 - \left(\frac{r_S}{r_K}\right)^2\right]^2 + 4\left(\frac{r_S}{r_K}\right)^2 \cdot \left(\frac{a}{r_K}\right)^2}\,\right]$$

$$\gamma = -(1 - p_1^2)/(a/r_K)$$

$$M^* = M\{(\gamma^2 \cdot i^2/r_K^2) + [1 - \gamma \cdot e/r_K]^2\}/(1 + \gamma^2)$$

$$i^* = i/r_K \cdot [\gamma(\gamma + e/r_K) + (1 - \gamma e/r_K)]/[\gamma^2 i^2/r_K^2 + (1 - \gamma e/r_K)^2]$$

$$e^* = [\gamma e^2/r_K^2 - (1 - \gamma e/r_K)(\gamma + e/r_K)]/[\gamma^2 i^2/r_K^2 + (1 - \gamma e/r_K)^2]. \quad (16)$$

It is evident that equation (15) has the same form as equation (1), hence it may be transformed into equation (5). In this case it is unlikely that:

$$(K_L + p_1^2 S_L)(K_L + p_2^2 S_L) = (K_L + p_2^2 S_L)(K_L + p_1^2 S_L) \quad (7a)$$

since by definition the two structural systems have different stiffness properties, so that it might appear that the two matrices $\mathbf{\Phi}_{Ro}^T M^* i^* \mathbf{\Phi}_{Lo}$ and $\mathbf{\Phi}_{Lo}^T M^* i^* \mathbf{\Phi}_{Ro}$ may not be predominantly diagonal. However, a large number of building structures analyzed by the authors showed that neglecting the off-diagonal terms in both models did not appreciably affect the natural frequencies and mode shapes (e.g. Table 3). This is to be expected, since the corresponding mode shapes of the two uncoupled systems, although different, are sufficiently close to render the diagonal terms larger than the off-diagonal ones. It therefore appears that the 2-d.f. model in equation (9) is sufficiently accurate for most practical purposes. Yet as with every approximate procedure, estimates of the expected errors are required. Such estimates may be obtained by means of a perturbation procedure[1] which is outlined in Appendix 1.

CALCULATION OF THE DYNAMIC EARTHQUAKE RESPONSE

Under earthquake excitation, the equation of motion associated with equations (15) or (1) may be written as

$$\mathfrak{M}^* \ddot{\mathbf{v}} + C^* \dot{\mathbf{v}} + \mathbf{K}^* \mathbf{v} = -\mathfrak{M}^* \mathbf{\Gamma}_s^{-1} \mathbf{r} \ddot{u}_g \quad (17)$$

in which $\mathbf{v}$ is the displacement response vector of order $2N$, C^* = Caughey type damping matrix [3], $\ddot{u}_g$ = the unidirectional earthquake acceleration time history, $\mathbf{r}$ is a vector of ones and zeros with the ones corresponding to the degree-of-freedom in the direction of $\ddot{u}_g$, $\mathbf{\Gamma}_s$ = the static modal participation matrix as defined in equation (14). Note that for the first model in which the system is statically uncoupled, $\mathbf{\Gamma}_S$ becomes a unit diagonal matrix.

The response $\mathbf{v}$ could be computed by a step-by-step integration of the matrix equation (17), and several techniques are available for this purpose (e.g. Ref. [5]). However, the normal mode approach combined with the response spectrum technique is much simpler and is sufficiently accurate for many practical applications. Following the normal mode procedure outlined in the preceding section, the displacements are first expressed terms of the uncoupled modal coordinates:

$$\mathbf{v} = \mathbf{\Phi}_o\, \mathbf{q} \quad (18)$$

in which $\mathbf{q}$ is the vector of modal coordinates amplitudes.

Then the approximate expression for the N 2×2 equations of motions are obtained as follows:

$$\begin{bmatrix} 1 & e^*/i^* \\ e^*/i^* & (e^*/i^*)^2+1 \end{bmatrix} \begin{Bmatrix} \ddot{q}_{Lj} \\ \ddot{q}_{Rj} \end{Bmatrix} + \begin{bmatrix} 2\omega_{Loj}\xi_{Lj} & 0 \\ 0 & 2\omega_{Roj}\xi_{Rj} \end{bmatrix} \begin{Bmatrix} \dot{q}_{Lj} \\ \dot{q}_{Rj} \end{Bmatrix} + \begin{bmatrix} \omega_{Loj}^2 & 0 \\ 0 & \omega_{Roj}^2 \end{bmatrix} \begin{Bmatrix} q_{Lj} \\ q_{Rj} \end{Bmatrix} = \begin{Bmatrix} \Gamma_{Lj} \\ \Gamma_{Rj} \end{Bmatrix} \ddot{u}_g \tag{19}$$

in which

$$\begin{Bmatrix} \Gamma_{Lj} \\ \Gamma_{Rj} \end{Bmatrix} = \begin{bmatrix} \boldsymbol{\phi}_{Loj}^T & \mathbf{0}^T \\ \mathbf{0}^T & \boldsymbol{\phi}_{Roj}^T \end{bmatrix} \mathfrak{M}^* \cdot \mathbf{\Gamma}_s^{-1} \cdot \mathbf{r} \tag{20}$$

is the vector of the modal participation factors. Note that, for $\boldsymbol{\phi}_{Lo} \equiv \boldsymbol{\phi}_{Ro} \cdot i$, equation (19) is exact and moreover, for the first model, where $\mathbf{\Gamma}_s \equiv I$, the right hand side becomes:

$$\begin{Bmatrix} \Gamma_{Lj} \\ \Gamma_{Rj} \end{Bmatrix} = \begin{Bmatrix} \Gamma_{Lj} \\ \Gamma_{Rj} \cdot e^*/i^* \end{Bmatrix} = \Gamma_{Loj} \begin{Bmatrix} 1 \\ e^*/i^* \end{Bmatrix} \tag{21}$$

in which Γ_{Loj} is the lateral modal participation factor. The 2-d.f. equation of motion given in equation (19) with its right hand side as given by equation (21) can be solved numerically for the prescribed acceleration $\ddot{u}_g$, for any set of $\omega_{Lj}, \omega_{Rj}, \xi_{Lj}, \xi_{Rj}$ and e^*/i^* to yield the maximum 2-d.f. response. Their maxima can then be combined in the RSS manner to obtain an estimate of maximum response of the system. This constitutes the 2-d.f. response spectra procedure proposed by Penzien[13, 14]. Since such spectra are not readily available, the standard 1-d.f. response spectra are used and the estimate of the maximum 2-d.f. response is obtained by the modified RSS formula proposed by Rosenblueth and Elorduy[15]. For this purpose equation (19) is uncoupled by means of the modal matrix of equation (11), which leads to:

$$\ddot{q}_{nj} + 2\omega_{nj} \cdot \xi_{nj} \cdot \dot{q}_{nj} + \omega_{nj}^2 q_{nj} = \Gamma_{nj}\ddot{u}_g \qquad (n=1,2) \tag{22}$$

in which Γ_{nj} are given by equation (20) and

$$\begin{Bmatrix} \Gamma_{1j} \\ \Gamma_{2j} \end{Bmatrix} = \mathbf{\Psi}_j^T \begin{Bmatrix} \Gamma_{Lj} \\ \Gamma_{Rj} \end{Bmatrix} \tag{23}$$

where $\mathbf{\Psi}_j$ is the approximate 2-d.f. modal matrix given in equation (11). The solution of each independent modal response equation (22) may be written as:

$$q_{nj} = \Gamma_{nj} S_{dnj} \qquad (n=1,2,\ j=1,N) \tag{24}$$

where S_d is the spectral displacement of $\ddot{u}_g$.

To obtain the modal lateral forces P and the modal torsional moments T at any reference level k of the structure, backward transformation is required, which leads to:

$$\begin{Bmatrix} P \\ T \end{Bmatrix}_{nj} = \mathfrak{M}^* \mathbf{\Phi}_o \boldsymbol{\psi}_{nj} \Gamma_{nj} S_{anj} \tag{25}$$

where S_a is the spectral acceleration. Explicitly, the components of the coupled j-th pair of the lateral forces are:

$$\begin{Bmatrix} P_1 \\ P_2 \end{Bmatrix}_j^k = \begin{Bmatrix} M^*\phi_{Loj}^K[\psi_{Lj1} + \psi_{Rj1} \cdot \alpha_j^k(e^*/i^*)]\Gamma_{1j}S_{a1j} \\ M^*\phi_{Loj}^K[\psi_{Lj2} + \psi_{Rj2} \cdot \alpha_j^k(e^*/i^*)]\Gamma_{2j}S_{a2j} \end{Bmatrix} \tag{26}$$

in which α_j^k is proportional to the ratio of k-th components of the noncoupled modal shapes and reads:

$$\alpha_j^k = i^* \cdot \phi_{Roj}^k / \phi_{Loj}^k \tag{27}$$

and the torsional moments are given by:

$$\begin{Bmatrix} T_1 \\ T_2 \end{Bmatrix}_j^k = \begin{Bmatrix} i^*M^*\phi_{Loj}^k[\psi_{Lj1}(e^*/i^*) + \alpha_j^k\psi_{Rj1}(e^*/i^*+1)]\Gamma_{1j}S_{a1j} \\ i^*M^*\phi_{Loj}^K[\psi_{Lj2}(e^*/i^*) + \alpha_j^k\psi_{Rj2}(e^{*2}/i^{*2}+1)]\Gamma_{2j}S_{a2j} \end{Bmatrix}. \tag{28}$$

For the static method of seismic analysis several building codes[7] require that the dynamic eccentricity due to modal coupling be computed. Denoting the dynamic eccentricity by e_d^* and the static eccentricity by e^*, the corrected 2-d.f. RSS amplification of the static eccentricity is given by[15]:

$$C_j = \frac{e_d^*}{e^*} = \frac{1}{e^*}\left[\frac{T_{1j}^2 + T_{2j}^2 + 2T_{1j} \cdot T_{2j}/(1+\varepsilon_{12j}^2)}{P_{1j}^2 + P_{2j}^2 + 2P_{1j}P_{2j}/(1+\varepsilon_{12j}^2)}\right]^{1/2} \tag{29}$$

in which the correction coefficient for close frequencies ε_{12j}, proposed by Rosenblueth and Elorduy[15] is:

$$\varepsilon_{12j} = \frac{|\omega_{1j}' - \omega_{2j}'|}{\omega_{1j}\xi_{1j}' + \omega_{2j}\xi_{2j}'} \tag{30}$$

where ω' designates the damped natural frequencies and ξ' the modified damping ratio.

The dynamic amplification factor C_j was evaluated numerically as a function of ω_{Ro}/ω_{Lo} for a large number of building structures. Since in general C_j^k is not constant but varies along the building height, its values were computed at a level where $\alpha_j^k = 1$, i.e. where $\phi_{Lo}^K = i^*\phi_{Ro}^K$. Figure 3 shows the dependence of C_j on the coupling parameter e^*/i^*, for the first model, using the spectrum shown in the insert. The continuous heavy line represents the exact 2-d.f. case and the dashed band shows the range of the results for the structures analyzed. These structures were chosen so as to produce large variations between their uncoupled lateral and torsional mode shapes. This was

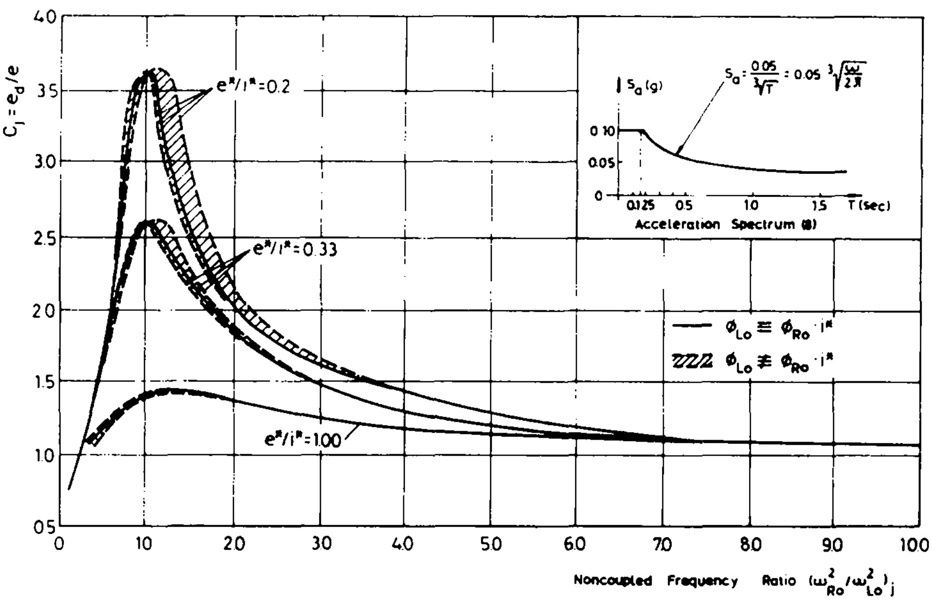

Fig. 3. Dynamic amplification factor.

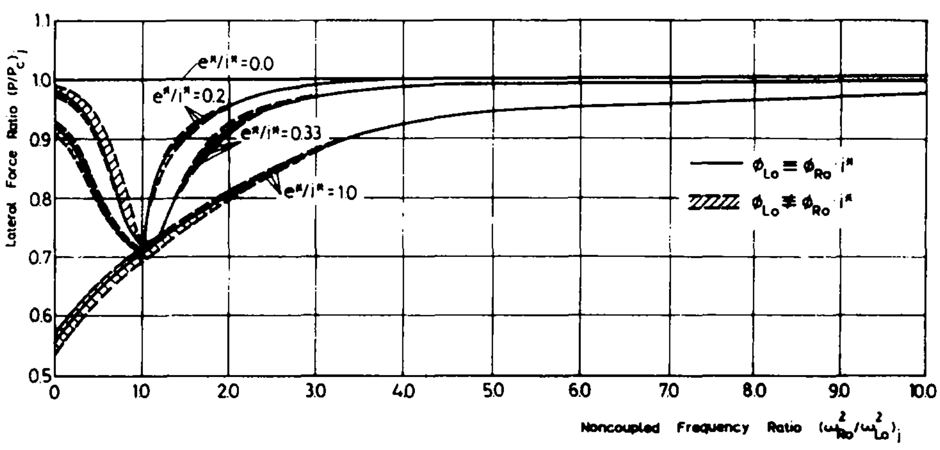

Fig. 4. Relation between dynamic and static lateral forces.

achieved by choosing uniform flexural cantilever properties for the one, and uniform shear cantilever properties for the other. It should be noted that the boundaries of the bands were plotted based on the exact and on the approximate solutions of the problems analyzed, so that the narrowness of the bands should give confidence in the proposed approximate solution. Figure 4 reveals an interesting feature of eccentric systems, namely the fact that while torsional coupling leads to the magnification of static eccentricity, it tends to lower the lateral shear forces. This phenomenon was first reported by Rosenblueth and Elorduy[15] for single story structures. No graphs are presented for the amplification factor of the second model. However, Figs. 3 and 4 may still be used with a suitable correction which is given in Appendix 2.

As already noted, another interesting feature of a structure in which $\Phi_{Lo} \neq \Phi_{Ro} i^*$ is the variation of the dynamic amplification factor C_j^k along the building height. As can be seen from equations (26, 28), C_j^k does not depend on α_j^k when e/i is large, and remains constant along the building height. For small values of e/i, the variation of C_j^k with height is proportional to the mode shape ratio α_j^k. This is of some practical importance, since an approximation for C_j^k at any level may be obtained by interpolating between the value of C_j as given in Fig. 3 and $C_j \cdot \alpha_j^k$. This can be seen in Fig. 6. In the following section two numerical examples are presented to illustrate the application of the proposed method.

NUMERICAL EXAMPLES

Example 1. The 43-story Wells Fargo building in San Francisco originally analyzed by Medearis[11] is used to illustrate the procedure (Fig. 5). The relevant structural properties are given below:

$K_x = K_y = 110\,280$ kip/ft (1.610×10^9 N/m);

$K_R = 495\,144000$ kip · ft/radian ($671,55 \times 10^9$ N · m/rad);

$M = 73.56$ kip s²/ft (1.073×10^6 kg);

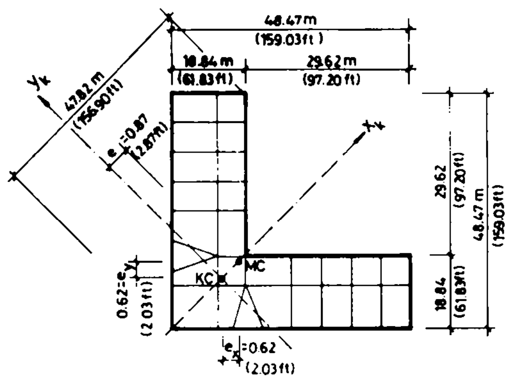

Fig. 5. Wells Fargo building framing system.

$i \;= 62.99$ ft (19.20 m);

$e_x \;= e_y = 2.03$ ft (0.619 m);

$K_L \;= K_x = K_y$;

$e \;= e_x \cdot \sqrt{2} = 2.87$ ft (0.785 m);

$r_K \;= (K_R/K_L)^{1/2} = 67.00$ ft (20.42 m).

The parameters required for the analysis are easily obtained from the above properties:

$$e/i = 0.0456; \qquad \omega_{Ro}/\omega_{Lo} = r_K/i = 1.06.$$

Free vibrations. Since the structural properties of this building satisfy equation (1) and equation (7) the 129-d.f. system can be reduced, due to symmetry, to a 43-d.f. system plus one 2-d.f. system. The 43-d.f. problem may then be further reduced to a single parameter continuous system if it is recognized that the structure is practically a uniform shear beam whose dynamic properties are well known[12]. To obtain the natural frequencies, equation (10) is used:

$$\left(\frac{\omega_{1,2}^2}{\omega_{Lo}^2}\right)_j = \tfrac{1}{2}[(1 + 1.06^2 + 0.0456)^2$$

$$\pm\sqrt{(1 - 1.06^2 + 0.0456^2)^2 + 4\cdot(0.0456\cdot 1.06)^2}]$$

$$= \begin{cases} 0.9859 \\ 1.1476 \end{cases}$$

so that for $\omega_{Lo_1} = 1.398$ rad/s and $\omega_{Lo_2} = 4.192$ rad/s:

$$\omega_1 = 1.398\sqrt{0.9859} = 1.388 \text{ rad/s } (1.388)$$

$$\omega_2 = 1.398\sqrt{1.1476} = 1.498 \text{ rad/s } (1.498)$$

$$\omega_3 = 4.192\sqrt{0.9859} = 4.162 \text{ rad/s } (4.163)$$

$$\omega_4 = 4.192\sqrt{1.1476} = 4.491 \text{ rad/s } (4.491).$$

The values in parentheses are those computed by Medearis from his 129-d.f. system. Using equations (11, 4) the coupled mode shapes are evaluated to yield:

$$\boldsymbol{\phi}_{1_j} = \begin{Bmatrix} 0.9541 & \boldsymbol{\phi}_{Lo_j} \\ 0.2996 & \boldsymbol{\phi}_{Lo_j}/i \end{Bmatrix}$$

$$\boldsymbol{\phi}_{2_j} = \begin{Bmatrix} 0.1566 & \boldsymbol{\phi}_{Lo_j} \\ -0.9425 & \boldsymbol{\phi}_{Lo_j}/i \end{Bmatrix} \qquad j = 1 \rightarrow 43.$$

Higher natural frequencies and their coupled mode shapes may be evaluated in a similar manner.

Forced response. The modal forces and torques are evaluated using equations (21, 26, 28):

$$\begin{Bmatrix} P_1 \\ P_2 \end{Bmatrix}_j = \begin{Bmatrix} 0.9365\, S_{a1j} \\ 0.1294\, S_{a2j} \end{Bmatrix} M\boldsymbol{\phi}_{Loj}\Gamma_{Loj} \tag{26}$$

$$\begin{Bmatrix} T_1 \\ T_2 \end{Bmatrix}_j = \begin{Bmatrix} 0.3327\, S_{a1j} \\ -0.1065\, S_{a2j} \end{Bmatrix} M_I\boldsymbol{\Phi}_{Loj}\Gamma_{Loj}. \tag{28}$$

Substituting these values in equation (29), the amplification of the static eccentricity for the spectrum given in Fig. 3 is obtained:

$$C_j = \left(\frac{e_d}{e}\right)_j = \frac{1}{0.0456} \times \left[\frac{0.3327^2 + 0.1065^2\cdot(S_{a2}/S_{a1})_j^2 - 0.3327\cdot 0.1065\cdot(S_{a2}/S_{a1})_j/1.58}{0.9365^2 + 0.0129^2\cdot(S_{a2}/S_{a1})_j^2 \quad 0.9365\cdot 0.0129\cdot(S_{a2}/S_{a1})_j/1.58}\right] \tag{29}$$

which for the first pair of coupled modes is:

$$C_1 = \left(\frac{e_d}{e}\right)_1 = \frac{1}{0.0456}\cdot\left[\frac{0.0996}{0.8850}\right]^{1/2} = 7.35.$$

For the higher pairs, the ratios of the spectral values are different, but the amplification factors remain practically unchanged.

The ratio of the computed lateral force P to the uncoupled lateral force P_c for the first pair is given by:

$$\left(\frac{P}{P_c}\right)_1 = \sqrt{0.8850}\left(\frac{S_{a1}}{S_{ao}}\right)_1 = 0.9387.$$

This ratio is practically unchanged for the higher modes, and it is evident that the effect of coupling on these forces is quite small. It follows that the RSS eccentricity magnification factor (C) as well as the RSS lateral force ratio (P/P_c) is quite accurately given by the results for the first pair of modes as given above. The dynamic eccentricity is found to be:

$$e_d = 7.35\cdot 0.9387\cdot 2.87 = 19.79 \text{ ft } (6.03 \text{ m}).$$

Comparing this result with a typical code provision as given by:

$$e_d = 1.5e + 0.05\, L_{max} = 12.15 \text{ ft } (3.70 \text{ m}).$$

It is seen that in this case even when the accidental eccentricity effect (the $0.05\,L_{max}$ term) is taken into consideration, code provisions substantially underestimate the amplification of eccentricity.

Table 1. Stiffness properties of elements in Fig. 2

	Frame properties ($*10^{-4}$ m^4)					Wall properties ($*$m^4)				
	$\boxed{1}$ $\boxed{2}$	$\boxed{3}$ $\boxed{4}$	$\boxed{5}$	① ② ③ ④			⑤		⑥	⑦
Stories	Exterior column I_x	Interior column I_x	Beams I_{xx}	I_x	I_x	I_x	I_y	I_{ω}*m6	I_x	I_x
1	2	3	4	5	6	7	8	9	10	11
0–4	71.458	142.916	34.662	1.067	0.003	4.169	9.893	16.667	0.003	1.067
4–10	57.214	114.427	34.622	1.067	0.003	4.169	9.893	16.667	0.003	1.067
10–16	26.042	52.084	18.984	1.067	0.003	4.169	9.893	16.667	0.003	1.067
16–20	18.984	37.968	18.984	1.067	0.003	4.169	9.893	16.667	0.003	1.067

Table 2. Noncoupled natural frequencies for Example 2

Mode No.	j	1	2	3	4	5
1	2	3	4	5	6	7
Noncoupled	ω_{Lo}	3.452	11.58	25.33	45.82	72.90
Frequencies (s^{-1})	ω_{Ro}	2.518	12.96	35.23	68.74	113.4

Table 3. Dynamic properties of structure in Fig. 2.

Mode No.		1	2	3	4	5	6	7	8	9	10
(1)	(2)	(3)	(4)	(5)	(6)	(7)	(8)	(9)	(10)	(11)	(12)
Natural circular frequency	exact	2.518	3.465	11.55	13.02	25.33	35.24	45.82	68.74	72.90	113.4
(s^{-1})	approx	2.518	3.465	11.55	13.02	25.33	35.24	45.82	68.74	72.90	113.4
Participation factor	exact	1.164	2.053	−1.001	−0.360	0.613	0.282	0.459	0.207	−0.359	−0.163
	approx	1.165	2.052	−0.999	−0.369	0.615	0.286	0.458	0.209	−0.358	−0.163
Error of approximated mode shape (%)	mean error	0.52%	0.57%	1.96%	2.94%	6.65%	6.16%	3.71%	2.05%	11.11%	0.40%
$\lvert\phi_{app}/\phi_{exact}-1\rvert*100$	standard deviation	0.69%	0.75%	4.52%	9.24%	10.97%	17.28%	5.78%	2.54%	26.09%	0.61%

Example 2. A twenty story wall-frame building whose floor plan is given in Fig. 2 is used to illustrate the analysis procedure for the second model. The story height is 3.00 m (9.84 ft) and the total height $H = 60.00$ m (196.85 ft). The stiffness properties of the frames and the walls are given in Table 1,

$$E = 2.5 \times 10^7\ \text{kN/m}^2\ (3.6 \times 10^6\ \text{psi}),$$

and the story mass $M = 274\ kg$ (18.78 $kip\,s^2/$ft).

The parameters required for the calculations are:

$$e/i = e/[(L_x^2 + L_y^2)/12]^{1/2} = 4.94/10.08 = 0.49$$

$$r_K/i = \left[\sum_{①}^{⑦} (I_{xj}r_{xj}^2 + I_{yj}r_{Yj}^2 + I_{\omega j}) \Big/ \sum_{①}^{⑦} I_{xj}\right]^{1/2} \Big/ i$$

$$= 12.86/10.08 = 1.28$$

$$a/r_K = 8.94/12.86 = 0.70$$

$$r_s/r_K = \left[\sum_{\boxed{1}}^{\boxed{5}} S_j r_{sj}^2 \Big/ \sum_{\boxed{1}}^{\boxed{5}} S_j\right]^{1/2} \Big/ r_K$$

$$= \left[\sum_{\boxed{1}}^{\boxed{5}} r_{sj}^2/5\right]^{1/2} \Big/ r_K = 5.66/12.86 = 0.44.$$

Using the relations in equation (16), the transformed parameters are found to be; $p_{1,2} = 1.245$; 0.356; $\gamma = -0.799$;

$M^* = 350.347.36$ kg (24.012 kip s^2/ft);

$i^* = 1.637$; $e^* = 0.0437$.

The natural frequencies of the two noncoupled systems are given in Table 2.

The dynamic properties and the response of the structure to earthquake excitation (using the spectrum in Fig. 3) were computed by the proposed approximate method and by a standard eigenvalue computer program.

The dynamic properties of the structure for the first ten modes are given in Table 3, the results under 'approx' are

Table 4. Amplification factors and lateral force ratios for structure in Fig. 2

Pair No.	(j)	1	2	3	4	5
(1)	(2)	(3)	(4)	(5)	(6)	(7)
$C_j = \frac{e_d^*}{e_s^*}$	exact	11.74	10.85	11.83	11.94	12.84
	approx	11.76	11.06	11.99	12.07	12.16
$\frac{P}{P_c}$	exact	0.973	1.075	1.046	1.039	1.037
	approx	0.974	1.075	1.046	1.039	1.037

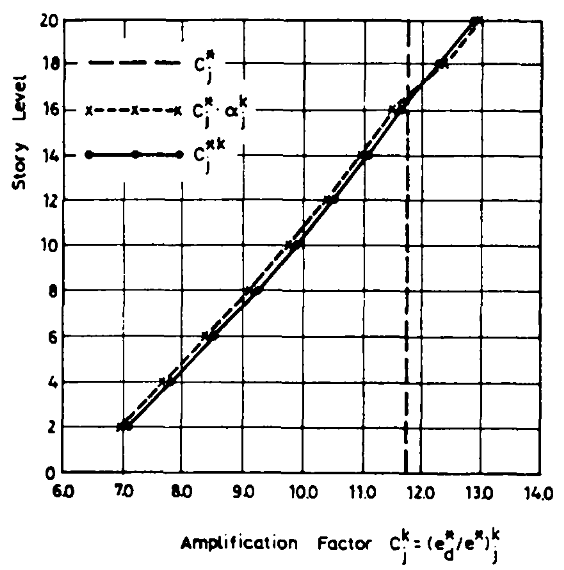

Fig. 6. Vertical variation of amplification factor (C_j^k); $j = 1$.

those obtained by the proposed method, whereas the values under 'exact' are these calculated using a lumped mass computer program. Comparing the result for the natural frequencies, modal participation factors and mode shapes, it is evident that the agreement is quite satisfactory. The large error in the shape of mode 9 is of no consequence since it is due to an error occurring at a zero-crossing of the mode shape.

The amplification factors and the lateral force ratios are given in Table 4 for the first five pairs of coupled modes. Again the agreement between the proposed method and the exact solution is quite satisfactory.

The variation of the eccentricity amplification factor along the height is of some interest. As mentioned in the foregoing section, this variation of the exact value is practically bracketed by C_j and by $C_j \cdot \alpha_j^k$. This is illustrated in Fig. 6 for the first pair of coupled modes $(j = 1)$.

SUMMARY AND CONCLUSIONS

An approximate method has been presented for the evaluation of the dynamic properties and the seismic response of a class of torsionally coupled multistory buildings. The solution is based on the similarity between the uncoupled lateral and torsional mode shapes which leads to a 2-d.f. representation of the coupling effect. The uncoupling of the system into two N d.f. systems plus N 2-d.f. systems is likely to reduce the complexity of computation substantially. An extensive parametric study has shown that the error involved using the method is sufficiently small and may be considered acceptable for earthquake analysis. Moreover, a check on the accuracy of the solution may be easily made by means of a perturbation analysis as outlined in Appendix 1.

The examples worked out demonstrate the limitations of the static methods of analysis for estimating the amplification of dynamic eccentricity. If such methods are to continue in use, the magnification factors stipulated by building codes should be made dependent on some basic coupling parameters at least for the range of internal resonance (Fig. 3). It has been shown that the 2-d.f. approximation as presented herein is likely to provide such parameters for a relatively large class of building structures. Outside this range the static amplification factors as given in the building codes may be used.

Nonlinear material behavior is to be expected during strong earthquakes, and in asymmetric structures it is associated with 'migration' of the rigidity axis. This subject merits further study.

REFERENCES

1. R. Bellman, *Introduction to Matrix Analysis*, McGraw-Hill, New York (1960).
2. J. I. Bustamente and E. Rosenblueth, Building code provision on torsional oscillations. *Proc. 2nd World Conf. Earthquake Engineering, Tokyo*. Vol. II, pp. 879–894 (1960).
3. T. Chaughey, Classical normal modes in damped linear systems. *J. Appl. Mech. Trans. ASME* **27**, 269–271 (1960).
4. R. W. Clough, Earthquake resistant design of tall buildings. *Proc. Symp. Tall Buildings, Planning, Design and Construction*. Nashville, Tenn., pp. 477 506 (1974).
5. A. Danay, J. Glück and M. Gellert, A generalized continuum method for dynamic analysis of asymmetric tall buildings. *Int. J. Earth. Engng Struct. Dyn.* **4** (2), 179–203 (1975).

6. G. W. Housner and H. Outinen, The effect of torsional oscillations on earthquake stresses, *Bull. Seis. Soc. Am.* **48**, 221–229 (1958).
7. *Earthquake Resistant Regulations of the World. A World List.* Int. Assoc. of Earthquake Engineering. Tokyo (1973).
8. Israeli Standard 413: *Characteristic Loads in Buildings: Earthquakes.* Israel Standards Institute. Tel-Aviv (1975).
9. C. L. Kan and K. A. Chopra, Earthquake response of a class of torsionally coupled buildings, *6th World Conf. Earth. Engng, New Delhi.* Preprints, Vol. 3, pp. 233–238 (1977).
10. E. Keintzel, On the seismic analysis of symmetrical storied buildings. *Proc. 5th World Conf. Earth. Engng Rome.* Vol. I, pp. 110–113 (1973).
11. K. Medearis, Coupled bending and torsional oscillations of a modern skyscraper. *Bull. Seis. Soc. Am.* **56**, 937–946 (1966).
12. N. M. Newmark and E. Rosenblueth, *Fundamentals of Earthquake Engineering*, Prentice Hall. Englewood Cliffs, N.J. (1971).
13. J. Penzien, Earthquake response of irregularly shaped buildings. *Proc. 4th World Conf. Earth. Engng. Chile.* Vol. II, A3 (1969).
14. J. Penzien and A. K. Chopra, Earthquake response of appendage on multistory building. *Proc. 3rd World Conf. Earth. Engng. New Zealand.* Vol. II, pp. 476–496 (1965).
15. E. Rosenblueth and E. Elorduy, Response of linear systems to certain transient disturbances. *Proc. 4th World Conf. Earth. Engng. Chile.* Vol. I, A-1, pp. 185–196 (1969).
16. A. Rutenberg and A. C. Heidebrecht, Approximate analysis of asymmetric wall-frame structures. *Build. Sci* **10**, 27–35 (1975).
17. A. Rutenberg, W. K. Tso and A. C. Heidebrecht, Dynamic properties of asymmetric wall-frame structures. *Int. J. Earth Engng Struct. Dyn.* **5**, 41–51 (1977).
18. R. I. Skinner, D. W. C. Skilton and D. A. Laws, Unbalanced buildings and buildings with light-towers under earthquake forces. *Proc. 3rd World Conf. Earth. Engng, New Zealand*, Vol. II, pp. 586–602 (1965).
19. A. Reinhorn, Influence of eccentricity between mass center and stiffness center on the dynamic response of storied structures. Report submitted to Technion – Israel Institute of Technology for Ph.D. Candidate requirements, Haifa, Israel, April (1975).
20. J. Glück and A. Reinhorn, Dynamic eccentricity of static equivalent earthquakes loads on asymmetric tall wall framed structures. Unpublished Report, Faculty of Civil Eng., Technion – Israel Institute of Technology, Haifa, Israel, September (1975).

APPENDIX 1

Perturbation analysis

Equation (5) may be rewritten in the form:

$$\left(\begin{bmatrix}\omega_{Lo} & 0\\ 0 & \omega_{Ro}^2\end{bmatrix} - \lambda\begin{bmatrix} I & I\,e/i\\ I\,e/i & I(1+e^2/i^2)\end{bmatrix} - \varepsilon\lambda \begin{bmatrix} 0 & (\boldsymbol{\Phi}_{Lo}^T M\, i\boldsymbol{\Phi}_{Ro} - I)e/i\\ (\boldsymbol{\Phi}_{Ro}^T M\, i\boldsymbol{\Phi}_{Lo} - I)e/i & 0\end{bmatrix}\right) \cdot \begin{Bmatrix}\boldsymbol{\psi}_L\\ \boldsymbol{\psi}_R\end{Bmatrix} = \begin{Bmatrix}0\\ 0\end{Bmatrix}$$

or:

$$(\boldsymbol{\omega}_0^2 - \lambda\boldsymbol{\mu} - \varepsilon\lambda\Delta\boldsymbol{\mu})\boldsymbol{\psi} = 0 \tag{31}$$

in which $\lambda = \omega^2$ is the eigenvalue and ε is a perturbation factor introduced in the above expression to facilitate grouping of terms with comparable degrees of approximation[1]. Comparing equation (31) with (8) shows that the unperturbed solution of equation (31) are those of equations is obtained (see e.g. [1]) of which the first order eigenvalue $\lambda_j = \omega_j^2$ and eigenvector $\boldsymbol{\psi}_j$ in terms of the powers of ε:

$$\lambda_j = \lambda_j^{(0)} + \varepsilon\lambda_j^{(1)} + \varepsilon^2\lambda_j^{(2)} \ldots \tag{32}$$

$$\boldsymbol{\psi}_j = \boldsymbol{\psi}_j^{(0)} + \varepsilon\boldsymbol{\psi}_j^{(1)} + \varepsilon^2\boldsymbol{\psi}_j^{(2)} \ldots \tag{33}$$

†Or similar in form if the diagonal terms rather than $I\,e/i$ are retained in the unperturbed solution – such an approach gives better estimates for the eigenparameters as can be easily verified from equation (36).

Substituting equation (32) and (33) into (31) and equating like powers of ε, a system of perturbation equations is obtained [see e.g. [1])] of which the first order one is given by:

$$(\boldsymbol{\omega}_0^2 - \lambda_j^{(0)}\boldsymbol{\mu})\boldsymbol{\psi}_j^{(1)} = \lambda_j^{(1)}\boldsymbol{\mu}\boldsymbol{\psi}_j^{(0)} + \lambda_j^{(0)}\Delta\boldsymbol{\mu}\boldsymbol{\psi}_j^{(0)}. \tag{34}$$

The first order correction of the eigenvector is now expressed as a linear combination of all the unperturbed eigenvectors and reads:

$$\boldsymbol{\psi}_j^{(1)} = \sum_{i=1}^{N} a_{ij1}\boldsymbol{\psi}_{i1}^{(0)} + \sum_{i=1}^{N} a_{ij2}\boldsymbol{\psi}_{i2}^{(0)}. \tag{35}$$

Note that the two sums represent the two vectors given in equation (11) and that each has only two non-zero elements. Substituting equation (35) in (34) premultiplying by $\boldsymbol{\psi}_i^{(0)T}$ and using the orthogonality properties of the normal modes, one obtains $\lambda^{(1)}$ and a_{ij} as follows:

$$\lambda_{jk}^{(1)} = -\lambda_{jk}^{(0)}\boldsymbol{\psi}_{jk}^{(0)T}\Delta\mu\boldsymbol{\psi}_{jk}^{(0)} \tag{36}$$

and

$$a_{ijk} = \frac{\lambda_{jk}^{(0)}}{\lambda_i^{(0)} - \lambda_{jk}^{(0)}}\boldsymbol{\psi}_i^{(0)T}\Delta\boldsymbol{\mu}\boldsymbol{\psi}_{jk}^{(0)} \quad k = 1, 2. \tag{37}$$

Note that a_{jj} is still undetermined. It is determined in the final solution by normalizing $\boldsymbol{\psi}_j$.

To obtain a second correction it is necessary to perform a second perturbation analysis. This again requires the expression of the eigenvector $\boldsymbol{\psi}_j^{(2)}$ in terms of the unperturbed vector $\boldsymbol{\psi}_i^{(0)}$. For details the reader may consult Ref. [17] in which a similar procedure for a continuous structure is given.

APPENDIX 2

Amplification of static eccentricity for second model

Comparing the right hand side of equation (21) with that of (20) it is seen that new loading terms are added to the second model. The modal participation factor Γ, then, takes the form:

$$\Gamma = \Gamma_a - \gamma i^* \Gamma_b \tag{38}$$

in which Γ_a and Γ_b are respectively dependent on the transformed 'lateral' and 'rotational' components of the excitation.

Using equations (26, 28) and (29) the eccentricity amplification factor C_j^* for the second model may be expressed as a function of C_j (given in Fig. 3) to read:

$$C_j^* = C_j \cdot \left[\frac{1 + (\gamma i^{*2}/C_j e^*)^2 \cdot \sum_{i=1}^{2} \Gamma_{ai}^4 \cdot (\eta_i^4 - 2\eta_i^3/\gamma i^*) \cdot \frac{S_{ai}^2}{S_{a1}^2} \Big/ \sum_{i=1}^{2} \Gamma_{ai}^4 \frac{S_{ai}^2}{S_{a1}^2}}{1 + (\gamma e^* C_j)^2 \sum_{i=1}^{2} \Gamma_{ai}^4 (\eta_i^2 - 2\eta_i/\gamma i^*) \cdot \frac{S_{ai}^2}{S_{a1}^2} \Big/ \sum_{i=1}^{2} \Gamma_{ai}^4 \eta_i^2 \frac{S_{ai}^2}{S_{a1}^2}} \right]^{1/2} \tag{39}$$

where

$$\begin{bmatrix} \Gamma_{ai} = \psi_{Li} + \psi_{Ri} e^*/i^* \\ \eta_i = \Gamma_{bi}/\Gamma_{ai} \\ \Gamma_{bi} = \psi_{Li} e^*/i^* + \psi_{Ri}[(e^*/i^*)^2 + 1] \end{bmatrix}.$$

Similarly the force ratio $(P/P_c)^*$ may be expressed as a function of P/P_c of the first model (Fig. 4):

$$(P/P_c)^* = (P/P_c) \left\{ 1 + [\gamma i^*/(P/P_c)]^2 \cdot \sum_{i=1}^{2} \Gamma_{ai}^3 (\eta_i^2 - 2\eta_i) \frac{S_{ai}^2}{S_{a1}^2} \right\}^{1/2}. \tag{40}$$

For small values of e^*/i^* it may be shown that:

$$C_j^* = C_j \{ [1 + (\gamma i^{*2}/C_j e^*)^2] / [1 + (\gamma e^* C_j)^2] \}^{1/2} \tag{41}$$

and

$$P/^*P_c = (P/P_c)\{1 + [\gamma i^*/(P/P_c)]\}^{1/2}.$$

When e^*/i^* is large, C_j^* and $(P/P_c)^*$ become equal to their first model counterparts.